Front. Phys., 2013, 8(3): 242–247
DOI 10.1007/s11467-013-0296-x

REVIEW ARTICLE

Overview on neutrinos and the Daya Bay experiment

Miao He

Division for Experimental Physics, The Institute of High Energy Physics, Chinese Academy of Sciences, Beijing 100049, China
E-mail: hem@ihep.ac.cn

Received December 3, 2012; accepted January 14, 2013

Neutrinos are elementary particles in the Standard Model. Neutrino oscillation is a quantum mechanical phenomenon beyond the Standard Model. Neutrino oscillation can be described by two independent mass-squared differences Δm^2_{21}, Δm^2_{31} (or Δm^2_{32}) and a 3×3 unitary matrix, containing three mixing angles θ_{12}, θ_{23}, θ_{13}, and one charge-parity (CP) phase. θ_{12} is about 34° and determined by solar neutrino experiments and the reactor neutrino experiment KamLAND. θ_{23} is about 45° and determined by atmospheric neutrino experiments and accelerator neutrino experiments. θ_{13} can be measured by either accelerator or reactor neutrino experiments. On Mar. 8, 2012, the Daya Bay Reactor Neutrino Experiment reported the first observation of non-zero θ_{13} with 5.2 standard deviations. In June, with 2.5× previous data, Daya Bay improved the measurement of $\sin^2 2\theta_{13} = 0.089 \pm 0.010(\text{stat}) \pm 0.005(\text{syst})$.

Keywords neutrino oscillation, neutrino mixing, Daya Bay

PACS numbers 14.60.Pq, 13.15.+g

Contents

1 Introduction to neutrino and neutrino oscillation

Neutrinos are elementary particles in the Standard Model. There are three flavors of neutrinos, known as ν_e, ν_μ and ν_τ. Neutrinos exist everywhere: the nuclear fusion in the sun, β-decays of radioactivities inside the Earth, the Big Bang remnant, the supernova explosion, or interactions between cosmic rays and the atmosphere of the Earth. Besides the natural sources, neutrinos can be also produced artificially in reactors and accelerators. The neutrino flavor states are superpositions of three mass eigenstates (ν_1, ν_2 and ν_3), which undergo quantum interference during the traveling, causing neutrino flavor changes. This phenomenon is known as neutrino oscillation. The amplitude of oscillation is connected to the mixing angles θ_{12}, θ_{23} and θ_{13}. The oscillation frequencies are determined by the difference of squared neutrino masses, $\Delta m^2_{ij} = m^2_i - m^2_j$.

As of one year ago, all of the mixing parameters had been measured except for θ_{13}. Solar neutrino experiments measured θ_{12} and Δm^2_{21}. Atmospheric neutrino experiments measured θ_{23} and $\left|\Delta m^2_{32}\right|$. The CHOOZ experiment set a limit of $\sin^2 2\theta_{13} < 0.17$ at 90% CL [1, 2] by the measurements of antineutrinos emitted from nuclear reactors. In 2011, two accelerator experiments T2K [3] and MINOS [4], and one reactor experiment Double Chooz [5], showed indication of none-zero θ_{13} at the level of 1 to 2.5 standard deviations.

In Mar. 2012, the Daya Bay Reactor Neutrino Experiment reported the first observation of non-zero θ_{13} with

5.2 standard deviations [6]. About one month later, the RENO experiment gave a consistent result with 4.9 standard deviations [7]. In June, with 2.5× previous data, Daya Bay has improved the measurement of θ_{13} [8].

2 θ_{12} and solar neutrino experiments

In the late 1960s, the Homestake [9] experiment observed a deficit in the flux of solar neutrinos with respect to the prediction from the Standard Solar Model. This experiment had been running for nearly 30 years, and the deficit persists [10], which is known as the solar neutrino problem. In 2001, the SNO [11] experiment detected neutrinos via both charge-current and neutral-current interactions, confirming that solar electron neutrinos do not disappear, but oscillate into the muon and tau flavors. The oscillation takes place inside the Sun through a matter-induced resonance known as MSW effect [12, 13]. Further measurements of the solar neutrino flux, as well as measurements of reactor neutrino flux by the KamLAND experiment, determined Δm^2_{21} and θ_{12}. The latest experiment values of these two oscillation parameters are $\Delta m^2_{21} = 7.50^{+0.19}_{-0.20} \times 10^{-5}$ eV^2, $\tan^2\theta_{12} = 0.452^{+0.035}_{-0.033}$ [14].

Recent results from Borexino [15–17], Super Kamiokande (Super-K) [18] and SNO [19] focused on low energy solar neutrinos between 1 MeV to 5 MeV. In this region, the solar neutrino disappearance is dominated by vacuum oscillation, compared to matter-enhanced oscillation in high energy range (> 5 MeV). These measurements not only improved the precision of oscillation parameters, but also confirmed the MSW effect and the Standard Solar Model.

3 θ_{23} and atmospheric neutrino experiments

The interaction of cosmic rays with the atmosphere of the Earth produces secondary particles, including hadrons and their decay products. In particular, pions produce neutrinos through the decay chain: $\pi \to \mu + \nu_\mu$, $\mu \to e + \nu_e + \nu_\mu$. Neutrinos from these interactions with energies from 100 MeV to about 100 GeV are called atmospheric neutrinos. The ratio of ν_μ to ν_e should be 2 at low energy range (< 1 GeV). Since 1980s, a few experiments measured this ratio and found it's smaller than the expectation [20], which is known as the atmospheric neutrino problem. In 1998, the Super-K experiment provided a very precise measurement of atmospheric ν_μ and ν_e flux, and found a deficit of ν_μ in the energy range of hundreds of MeV to a few GeV, at a distance of the diameter of the earth, which can be explained by a $\nu_\mu \to \nu_\tau$ oscillation. θ_{23} and $|\Delta m^2_{\rm atm}|$ (which is an approximation of $|\Delta m^2_{32}|$) were determined accordingly [21].

Muon neutrinos can also be produced in accelerators with a high intensity, which give a good opportunity for neutrino oscillation study. Recently, the MINOS experiment, using the neutrino beam in the Fermilab, updated the result of θ_{23} and $|\Delta m^2_{\rm atm}|$, by measuring the disappearance of ν_μ or $\overline{\nu}_\mu$ at a distance of 735 km. $|\Delta m^2_{\rm atm}| = 2.39^{+0.22}_{-0.27} \times 10^{-3}$ eV^2, $\sin^2 2\theta_{23} = 0.96^{+0.04}_{-0.04}$ in the neutrino mode, and $|\Delta m^2_{\rm atm}| = 2.48^{+0.22}_{-0.27} \times 10^{-3}$ eV^2, $\sin^2(2\theta_{23}) = 0.97^{+0.03}_{-0.08}$ in the antineutrino mode [22]. So the muon antineutrino disappearance is in good agreement with the neutrino result, which gives no indication of charge-parity-time reversal (CPT) violation.

4 θ_{13} in accelerator experiments

Besides determining θ_{23} and $|\Delta m^2_{\rm atm}|$, neutrinos from accelerators can also be used to measure θ_{13}, as well as studies of CP violation and the mass ordering of ν_2 and ν_3. The probability of muon neutrinos translating to electron neutrinos can be described as

$$\begin{aligned} P(\nu_\mu \to \nu_e) = {} & \sin^2(2\theta_{13}) \sin^2\theta_{23} \sin^2(1.27\Delta m^2_{31} L/E) \\ & +(\text{solar term}) \\ & +(\text{CP violation term}) \\ & +(\text{CP conservation term}) \\ & +(\text{matter effect term}) \end{aligned} \tag{1}$$

where Δm^2_{31} can be approximated by $\Delta m^2_{\rm atm}$, E is the neutrino energy in GeV and L is the distance in km between the neutrino source and the detector (baseline). The matter effect term can be enhanced with longer baseline, which gives the information of the mass ordering (mass hierarchy) of ν_2 and ν_3.

The T2K experiment uses the Super-K detector to detect neutrinos from J-PARC facility in Tokai, which is 295 km away from the detector. In Jun. 2011, T2K announced the observation of six electron neutrinos compared to an expected background of 1.5, which gives an indication of none-zero θ_{13} with a significance of 2.5 standard deviations [3]. Soon thereafter, the MINOS experiment reported their first result of θ_{13}, which also favors none-zero θ_{13}, and the significance is 1.7 standard deviations [4]. Both of T2K and MINOS gave an updated measurement of θ_{13} in Jun. 2012 with more statistics, and improved the significance to 3.2 [23] and 2.0 [24] standard deviations, respectively.

5 θ_{13} in reactor experiments

For reactor-based experiments, θ_{13} can be extracted from the survival probability of the electron antineutrino at a distance of 1–2 km from the reactors

$$P(\overline{\nu}_e \rightarrow \overline{\nu}_e) \approx \sin^2(2\theta_{13}) \sin^2(1.27\Delta m^2_{31} L/E) \qquad (2)$$

where E is the $\overline{\nu}_e$ energy in MeV and L is the distance in meters between the $\overline{\nu}_e$ source and the detector (baseline).

The past reactor experiments, such as Palo Verde [25] and CHOOZ [1], measured the neutrino flux with a single detector, and compared it with predictions from the reactor neutrino flux model, to get the oscillation probability. The sensitivity of such an absolute measurement is low due to large uncertainties from reactors and detectors. A relative measurement by detectors at two distances was proposed [26] to improve the sensitivity to oscillation due to θ_{13}. There are three ongoing reactor experiments using the method of multiple detectors: Daya Bay, Double Chooz, and RENO. The baselines of their far detectors are 1.65 km, 1.05 km, 1.44 km, respectively. Table 1 shows the comparison of their reactor power, detector(Det.) target mass in near/far(N/F) site, overburden and estimated sensitivity of θ_{13} measurement after 3 years of data taking.

Table 1 Comparison of three reactor experiments [27].

Exp.	Power GW	Det.(t) N/F	Overburden (m.w.e) N/F	3yr Sens. (90% C.L.)
DYB1)	17.4	40/80	250/860	0.008
DC2)	8.5	8/8	120/300	0.03
RENO	16.5	16/16	120/450	0.02

1) Daya Bay (DYB) had six detector modules running before Aug. 2012, so the detector mass was 20 ton less in near and far sites.

2) The near detector of Double Chooz (DC) will be running by the end of 2013.

In Nov. 2011, Double Chooz reported their first result of θ_{13} based on the measured neutrino rate in the far detector. It excludes vanishing θ_{13} at 1.7 standard deviations [5]. A shape analysis of the neutrino energy spectrum was applied later to reduce systematic uncertainties. In Jun. 2012, the updated result improved the significance to 2.9 standard deviations [28] with more data. The result of RENO was reported in Apr. 2012 with a measurement of antineutrinos in both near and far detectors. Details of Daya Bay experiment will be introduced in the next section.

6 The Daya Bay experiment

The Daya Bay experiment was designed to provide the most precise measurement of θ_{13} among existing and near future experiments, with a sensitivity to $\sin^2(2\theta_{13}) < 0.01$ at the 90% C.L. [29].

6.1 Experiment site

The experiment is located near Daya Bay, Ling Ao and Ling Ao-II nuclear power plants in southern China, 45 km from Shenzhen city. As shown in Fig. 1, there are six functionally identical reactor cores, grouped into three pairs. The last core started commercial operation by the middle of 2011. Three underground experimental halls (EHs) are connected with horizontal tunnels. Before Aug. 2012, six functionally identical antineutrino detectors (ADs) were installed. Two of them were located in EH1, one in EH2, and three near the oscillation maximum in EH3 (the far hall). The distances from the six ADs to the six cores were surveyed with the Global Positioning System (GPS) and with modern theodolites, resulting in a precision of 18 mm.

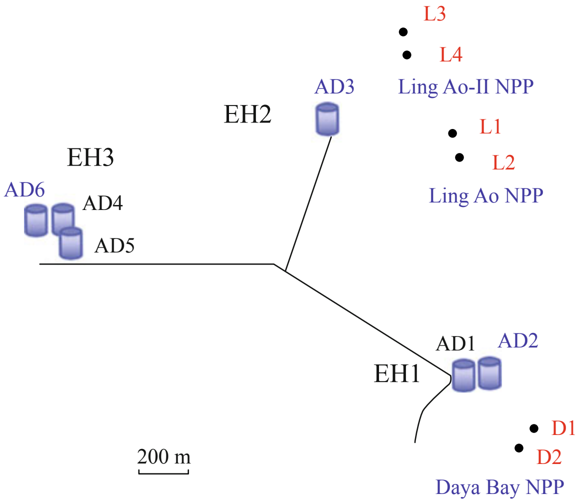

Fig. 1 Layout of the Daya Bay experiment. The dots represent reactor cores, labeled as D1, D2, L1, L2, L3 and L4. Six antineutrino detectors (AD1–AD6) were installed in three experimental halls (EHs).

6.2 Detectors

The $\overline{\nu}_e$ interacts with proton via the inverse β-decay (IBD) reaction in gadolinium-doped liquid scintillator (Gd-LS), and releases a e^+ and a neutron. The e^+ deposits its energy quickly, providing a prompt signal. The energy of e^+ carries most of the kinetic energy of the neutrino. The neutron is captured by Gd after an average time of ~30 μs, then releases several gammas with a total energy of ~8 MeV, providing a delayed signal. The coincidence of prompt-delayed signals provides a distinctive $\overline{\nu}_e$ signature.

Each experimental hall is equipped with ADs and muon veto system. Figure 2 shows a typical detector configuration taking EH1 as an example. Each AD is made of three nested cylindrical volumes separated by concentric acrylic vessels. The inner volume is filled with 20 t of Gd-LS with 0.1% Gd by weight and serves as the antineutrino target. The middle volume holds 20 t undoped liquid scintillator (LS), for detecting gammas that escape from the target. The outer volume contains 37 t of mineral oil (MO) to protect Gd-LS and LS from radioactivities. There are 192 8-inch photo-multiplier tubes (PMTs) installed inside the mineral oil, to detect the optical photons from the neutrino interaction in the detector.

The muon veto system consists of a water shield and a resistive plate chamber (RPC). The water pool is divided into two parts, and equipped with PMTs in each part, forming inner (IWS)and outer (OWS) cherenkov detectors. The resistive plate chamber contains $9 \times 6(9 \times 9)$ modules in the near(far) site. Each module has four layers with alternating orientated readout strips providing a spatial resolution of ~8 cm.

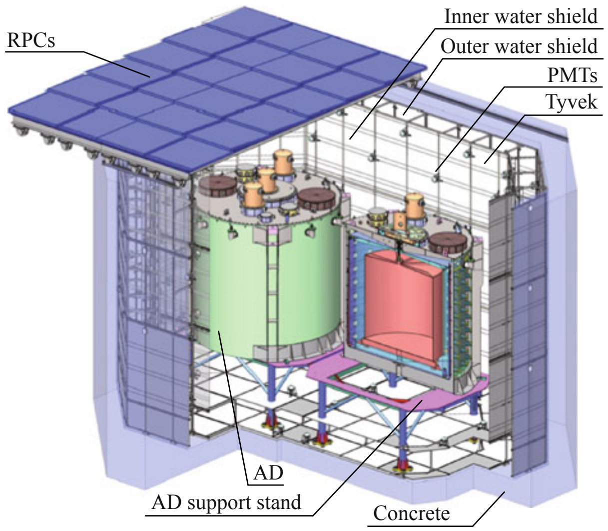

Fig. 2 The Daya Bay detectors.

6.3 Data analysis

The number of detected antineutrinos N_{det} is given by

$$N_{det} = \frac{N_p}{4\pi L^2} \int \epsilon \sigma P_{sur}(E, L, \theta_{13}) S \mathrm{d}E \tag{3}$$

where N_p is the number of free protons in the target, L is the distance of the detector from the reactor, ϵ is the efficiency of detecting an antineutrino, σ is the total cross-section of the IBD process, P_{sur} is the $\overline{\nu}_e \rightarrow \overline{\nu}_e$ survival probability that depends on the value of $\sin^2 2\theta_{13}$, and S is the differential energy distribution of the antineutrino.

For a single reactor core and single near and far detectors, the ratio of the number of antineutrino events with energy E detected at distance L_f (far detector) from the reactor core to that at a distance L_n (near detector) is given by

$$\frac{N_f}{N_n} = \left(\frac{N_{p,f}}{N_{p,n}}\right) \left(\frac{L_n}{L_f}\right)^2 \left(\frac{\epsilon_f}{\epsilon_n}\right) \left[\frac{P_{sur}(E, L_f, \theta_{13})}{P_{sur}(E, L_n, \theta_{13})}\right] \tag{4}$$

where $N_{p,f}$ and $N_{p,n}$ refer to the number of target protons at the far and near sites, respectively. The reactor neutrino flux and IBD cross-section are totally canceled, and the relative detector efficiency (ϵ_f/ϵ_n) can be determined more precisely than the absolute efficiency.

The IBD process is identified as a prompt-delayed pair, by requiring $0.7 < E_p < 12$ MeV, $6 < E_d < 12$ MeV, and $1 < \Delta t < 200$ μs, where E_p is the energy of prompt signal, E_d is the energy of delayed signal, Δt is the time interval between two signals. To remove backgrounds introduced by cosmic ray muons, the IBD candidate is removed if it follows a muon tagged by water shield or AD. A multiplicity cut requires no other > 0.7 MeV event 200 μs before the prompt signal or 200 μs after the delayed signal. Using 127 days data taken from Dec. 24, 2011 to May 11, 2012, a total number of 234 217 antineutrino candidates were measured by the six detectors.

The total residual backgrounds is 1.9% at the near halls and 4.7% at the far hall. The dominate background is accidentals, coming from two uncorrelated background radiation interactions that randomly satisfy the energy and time correlation for inverse β-decay antineutrino selection. It can be calculated by measuring the rate of both prompt- and delayed-type signals, and then estimating the probability of their accidental coincidences. The dominate uncertainty of background is from two sources of correlated signals. One is cosmogenic β-n isotope ^{9}Li/^{8}He, which can be measured by the time interval to previous muons. The other is from Am-C neutron calibration sources, which is estimated by Monte Carlo simulations, and constrained by the measurement of single event rate from Am-C sources. Other backgrounds such as fast neutrons produced by cosmic ray muons and $^{13}\mathrm{C}(\alpha, n)^{16}\mathrm{O}$ nuclear interactions are negligible in comparison. The total uncertainty of backgrounds is 0.2% at the near halls and 0.35% at the far hall.

The expected antineutrino rate in each AD can be obtained from the reactor neutrino flux, the neutrino interaction in the target and the detection efficiency. The reactor neutrino flux is calculated from the simulated fission rate and the antineutrino spectrum per fission of four main isotopes. The thermal power data were provided by the power plant. The target mass is measured during filling of GD-LS and the liquid level is monitored during the detector running. The uncorrelated uncertainty among ADs is 0.03%. The absolute efficiency is mainly given by the Monte Carlo study, and the uncertainty is 1.9%. In a relative measurement, only the uncorrelated uncertainty is considered, which is 0.2% determined with a side-by-side comparison of ADs [30].

A blind analysis strategy is adopted for the prediction of the antineutrino rate. The true value of reactor power, baseline and target mass is blinded till the analysis algorithms and parameters are fixed, to avoid unintended biasing of a result in a particular direction.

6.4 Experiment result

Antineutrino rates in the near detectors were used to predict the rates in the far detectors assuming no oscillation. The far detectors found $0.944 \pm 0.007(\text{stat}) \pm 0.003(\text{syst})$ of the expected flux relative to the near sites. An analysis of the relative antineutrino rates of the six detectors in a standard three-flavor oscillation model found $\sin^2(2\theta_{13}) = 0.089 \pm 0.010(\text{stat}) \pm 0.005(\text{syst})$, as shown in Fig. 3.

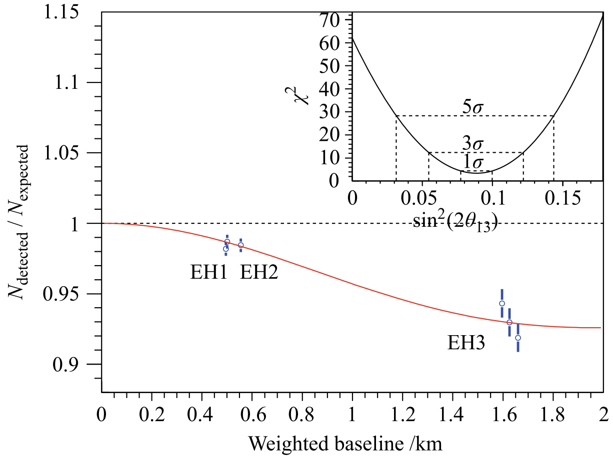

Fig. 3 A comparison of the measured antineutrino rates in the three near and three far detectors. In absence of oscillation, all points should lie on a horizontal line. The curve shows the relative antineutrino rates due to the best estimate of $\sin^2(2\theta_{13}) = 0.089$ in a three-flavor oscillation model.

A comparison of $\sin^2(2\theta_{13})$ measurements from different experiments is shown in Fig. 4. Using different neutrino sources such as solar neutrinos, accelerator neutrinos and reactor neutrinos, all of the experiments give consistent results.

7 Other neutrino experiments

Besides the three-flavor neutrino oscillation study, there are many other interesting topics and progresses related to neutrino experiments. An unexpected neutrino oscillation mode was reported in both accelerator and reactor experiments, known as the LSND anomaly [32] and reactor anomaly [33]. This phenomenon requires a new type of neutrinos called sterile neutrinos, which becomes a hot topic in neutrino physics. Geo-neutrinos produced in the Earth are good tools to study how the earth's interior works. In 2010, Borexino [34] and KamLAND [35] improved the significance of geo-neutrino measurements to better than 4 standard deviations, which is revealing more information about the Earth's heat production. The absolute mass of neutrinos can be measured by the end point of the electron energy spectrum in β-decays. The KATRIN [36] experiment aims for 0.93 eV energy resolution at the end point of 18.6 keV, corresponding to a sensitivity of 200 meV to the effective electron neutrino mass. On the other hand, an effective Majorana mass of neutrinos can be obtained from the measurement of the half-life of the neutrino-less double-β decay. This measurement may also answer the nature of massive neutrinos. In 2012, the EXO experiment [37] and the KamLAND-Zen experiment [38] obtained a lower limit for the neutrino-less double-β decay half-life as 16×10^{24} yr. and 5.7×10^{24} yr. at 90% CL, corresponding to a upper limit of 140–380 meV and 300–600 meV for the Majorana mass, respectively.

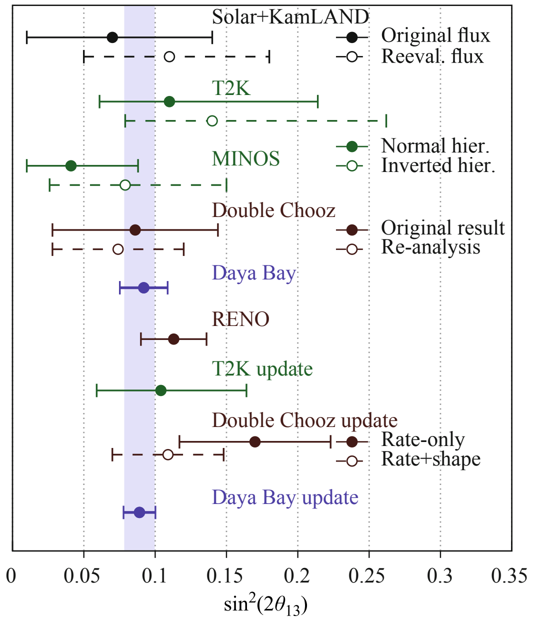

Fig. 4 A global picture of θ_{13} measurement [31].

8 Summary and prospective

There was significant progress in the understanding of the neutrino in the past years. After the Daya Bay experiment measured θ_{13}, all three mixing angles which determine the amplitudes of neutrino oscillations are known. Large θ_{13} makes it easier for the next generation neutrino experiments to determine neutrino mass hierarchy and search for CP violation in neutrino oscillations. The latter may answer the question that why there is more matter than antimatter in the Universe.

Acknowledgements The work was supported by the National Natural Science Foundation of China (Grant No. Y2118M005C). I would like to acknowledge the Daya Bay collaborators for useful comments, especially Prof. Jun Cao and Dr. Yufeng Li who helped

me a lot to improve this article.

References and notes

1. M. Apollonio, et al. [CHOOZ Collaboration], Phys. Lett. B, 1999, 466(2–4): 415
2. M. Apollonio, et al. [CHOOZ Collaboration], Eur. Phys. J. C, 2003, 27: 331
3. K. Abe, et al. [T2K Collaboration], Phys. Rev. Lett., 2011, 107(4): 041801
4. P. Adamson, et al. [MINOS Collaboration], Phys. Rev. Lett., 2011, 107(18): 181802
5. Y. Abe, et al. [Double Chooz Collaboration], Phys. Rev. Lett., 2012, 108(13): 131801
6. F. P. An, et al. [Daya Bay Collaboration], Phys. Rev. Lett., 2012, 108(17): 171803
7. J. K. Ahn, et al. [RENO Collaboration], Phys. Rev. Lett., 2012, 108(19): 191802
8. F. P. An, et al. [Daya Bay Collaboration], Chin. Phys. C, 2013, 37: 011001, arXiv: 1210.6327
9. R. Davis, D. S. Harmer, and K. C. Hoffman, Phys. Rev. Lett., 1968, 20(21): 1205
10. B. T. Cleveland, T. Daily, R. Jr Davis, J. R. Distel, K. Lande, C. K. Lee, P. S. Wildenhain, and J. Ullman, Astrophys. J., 1998, 496(1): 505
11. Q. R. Ahmad, et al. [SNO Collaboration], Phys. Rev. Lett., 2001, 87(7): 071301
12. L. Wolfenstein, Phys. Rev. D, 1978, 17(9): 2369
13. S. P. Mikheev and A. Yu. Smirnov, Sov. J. Nucl. Phys., 1985, 42: 913
14. A. Gando, et al. [The KamLAND Collaboration], Phys. Rev. D, 2011, 83(5): 052002
15. G. Bellini, et al. [Borexino Collaboration], Phys. Rev. D, 2010, 82(3): 033006
16. G. Bellini, et al. [Borexino Collaboration], Phys. Rev. Lett., 2011, 107(14): 141302
17. G. Bellini, et al. [Borexino Collaboration], Phys. Rev. Lett., 2012, 108(5): 051302
18. K. Abe, et al. [Super-Kamiokande Collaboration], Phys. Rev. D, 2011, 83(5): 052010
19. B. Aharmim, et al. [SNO Collaboration], arXiv: 1109.0763, 2011
20. W. Anthony Mann, arXiv: hep-ex/9912007v2, 1999
21. Y. Fukuda, et al. [Super-Kamiokande Collaboration], Phys. Rev. Lett., 1998, 81(8): 1562
22. P. Adamson, et al. [The MINOS Collaboration], Phys. Rev. Lett., 2012, 108(19): 191801
23. T. Nakaya, Plenary talk at the XXV International Conference on Neutrino Physics and Astrophysics, Kyoto, Jun. 2012
24. R. Nichol, Plenary talk at the XXV International Conference on Neutrino Physics and Astrophysics, Kyoto, Jun. 2012
25. F. Boehm, J. Busenitz, B. Cook, G. Gratta, H. Henrikson, J. Kornis, D. Lawrence, K. B. Lee, K. McKinny, L. Miller, V. Novikov, A. Piepke, B. Ritchie, D. Tracy, P. Vogel, Y. F. Wang, and J. Wolf, Phys. Rev. Lett., 2000, 84(17): 3764
26. L. A. Mikaelyan and V. V. Sinev, Phys. Atom. Nucl., 2000, 63: 1002, arxiv: hep-ex/9908047
27. J. Cao, Plenary talk at the 36th International Conference on High Energy Physics, Melbourne, Jul. 2012.
28. Y. Abe, et al. [Double Chooz Collaboration], arXiv: 1207.6632, 2012
29. DayaBay Collaboration, arxiv: hep-ex/0701029, 2007
30. F. P. An, et al. [Daya Bay Collaboration], Nucl. Inst. And Meth. A, 2012, 685: 78
31. S. Jetter, Plenary talk at the First International Conference on new Frontiers in Physics, Crete, Jun. 2012
32. A. Aguilar, et al. [LSND Collaboration], Phys. Rev. D, 2001, 64(11): 112007
33. G. Mention, M. Fechner, T. Lasserre, T. Mueller, D. Lhuillier, M. Cribier, and A. Letourneau, Phys. Rev. D, 2011, 83(7): 073006
34. G. Bellini, J. Benziger, S. Bonetti, M. B. Avanzini, et al., Phys. Lett. B, 2010, 687(4–5): 299
35. A. Gando, Y. Gando, K. Ichimura, H. Ikeda, et al., Nat. Geosci., 2011, 4(9): 64
36. F. M. Fraenkle, arXiv: 1110.0087, 2011
37. M. Auger, et al. [EXO Collaboration], Phys. Rev. Lett., 2012, 109(3): 032505
38. A. Gando, et al. [KamLAND-Zen Collaboration], Phys. Rev. C, 2012, 85(4): 045504